

Gallium vacancy complexes as a cause of Shockley-Read-Hall recombination in III-nitride light emitters

Cyrus E. Dreyer,^{1,a)} Audrius Alkauskas,^{2,3} John L. Lyons,^{1,b)} James S. Speck,¹ and Chris G. Van de Walle¹

¹Materials Department, University of California, Santa Barbara, California 93106, USA

²Center for Physical Sciences and Technology, Vilnius LT-01108, Lithuania

³Department of Physics, Kaunas University of Technology, Kaunas LT-51368, Lithuania

(Received 29 October 2015; accepted 12 February 2016; published online 4 April 2016)

We describe a mechanism by which complexes between gallium vacancies and oxygen and/or hydrogen act as efficient channels for nonradiative recombination in InGaN alloys. Our identification is based on first-principles calculations of defect formation energies, charge-state transition levels, and nonradiative capture coefficients for electrons and holes. The dependence of these quantities on alloy composition is analyzed. We find that modest concentrations of the proposed defect complexes ($\sim 10^{16} \text{ cm}^{-3}$) can give rise to Shockley-Read-Hall coefficients $A = (10^7 - 10^9) \text{ s}^{-1}$. The resulting nonradiative recombination would significantly reduce the internal quantum efficiency of optoelectronic devices. © 2016 AIP Publishing LLC. [<http://dx.doi.org/10.1063/1.4942674>]

Group-III nitrides are the key materials for light-emitting diodes (LEDs) in the blue part of the visible spectrum, which are used for general lighting applications.¹ A large research effort is aimed at extending this success to the green and the yellow range, where nitride LEDs are significantly less efficient. Internal quantum efficiency (IQE) is limited by recombination via defect states, the so-called Shockley-Read-Hall (SRH) recombination,^{2,3} and by Auger recombination.^{4,5} Within the so-called *ABC* model for IQE, the maximum efficiency is $B/(B + 2\sqrt{AC})$, where A is the SRH recombination coefficient, B is the radiative coefficient, and C is the Auger coefficient. Since B and C are intrinsic parameters of the bulk material, peak device efficiencies are determined by A . Experimental determination of the microscopic mechanism of SRH is complicated by the fact that the SRH rate depends on many parameters, including temperature, carrier concentration, non-uniformity of carrier distribution, type of material (bulk versus epitaxial), growth method, strain, polarization fields, and In content.

Gallium vacancy (V_{Ga}) complexes have been observed in GaN^{6,7} and proposed as recombination centers.^{8,9} In this work, we identify a microscopic mechanism of SRH recombination based on V_{Ga} complexed with O and/or H. The approach is based on accurate first-principles calculations and our recently developed methodology for nonradiative capture coefficients.¹⁰ For InGaN alloys that emit in the green and yellow, we demonstrate that these defects have SRH rates comparable or larger than radiative recombination rates, resulting in significantly reduced IQEs for devices.

Defect-assisted recombination in a material with a band gap E_g consists of sequential capture of an electron and a hole (or vice versa). For the example of a defect with a single (+1/0) charge-state transition level (Fig. 1), electron (hole)

capture is given by the rate $R_n = C_n N^+ n$ ($R_p = C_p N^0 p$), where n (p) is carrier density, N^+ (N^0) is the concentration of defects in the pertinent charge state, and C_n (C_p) is the capture coefficient. This coefficient encapsulates the propensity for the defect to capture the carrier and is often expressed as a capture cross-section multiplied by a characteristic velocity.¹¹

Expressions for the resulting recombination rate were derived by Shockley and Read,² as well as Hall.³ Assuming injected carrier densities $n = p$, SRH recombination is characterized by a rate $R_{\text{SRH}} = An$.^{4,5} For a defect density N , and omitting reemission of carriers from defect states to the band edges (which is negligible for deep levels in wide-band-gap materials)^{2,3}

$$A = N \frac{C_n C_p}{C_n + C_p}. \quad (1)$$

Therefore, in order to determine A , one needs to calculate electron and hole capture coefficients $C_{\{n,p\}}$ and estimate defect concentrations N . Based on positron annihilation⁶ and mobility¹² studies, we conservatively assume $N = 10^{16} \text{ cm}^{-3}$.

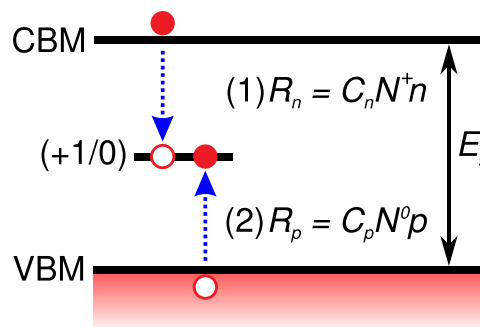


FIG. 1. Schematic energy band diagram depicting SRH recombination at a (+1/0) defect level in a material with band gap E_g . If the defect is initially in a +1 charge state, recombination proceeds via (1) electron capture with rate R_n and (2) hole capture with rate R_p . C_n (C_p) are capture coefficients, N^+ (N^0) the density of defects in the +1 (0) charge state, and n (p) the density of electrons (holes).

^{a)}Current address: Department of Physics and Astronomy, Rutgers University, Piscataway, New Jersey 08845-0849, USA. Electronic mail: cedreyer@engineering.ucsb.edu.

^{b)}Current address: Center for Functional Nanomaterials, Brookhaven National Laboratory, Upton, New York 11973, USA.

Experimentally observed A values that are known to impact device efficiency are on the order 10^6 – 10^7 s $^{-1}$.^{4,13,14} Given the assumed defect densities, the capture coefficients of relevant defects must therefore be $C_{\{n,p\}} = 10^{-10}$ – 10^{-9} cm 3 s $^{-1}$.

SRH recombination in principle covers both radiative and nonradiative capture at defects. Processes that rely on a radiative transition as the rate-limiting step will not contribute, given that typical values of radiative capture coefficients in GaN are 10^{-14} – 10^{-13} cm 3 s $^{-1}$.¹⁵ We thus search for a process where both hole and electron capture occur nonradiatively via the process of multiphonon emission.¹¹ We calculate $C_{\{n,p\}}$ completely from first principles following the methodology of Ref. 10. The capture coefficients depend strongly (approximately exponentially) on the energy of the transition. Other defect properties, such as effective phonon frequencies^{10,16} and electron-phonon coupling constants,¹⁰ affect the rates more weakly and do not significantly differ between the defects considered here. The bottom line is that only defects with transition levels within 1.5 eV of a band edge will result in nonradiative capture coefficients greater than 10^{-10} cm 3 s $^{-1}$. Combined with the fact that the overall recombination rate is governed by the slower of the electron and hole processes [Eq. (1)], our search is thus constrained to defects with levels near mid gap.

Our defect calculations are performed within the framework of density functional theory¹⁷ using the Vienna *Ab initio* Simulation Program VASP.¹⁸ We use the Heyd-Scuseria-Ernzerhof (HSE) hybrid functional¹⁹ with a fraction of screened Fock exchange $\alpha=0.31$; this approach accurately reproduces the band structure of GaN, which is essential for obtaining reliable defect levels.¹⁷ Atomic cores were treated within the projector augmented wave (PAW) approach. Formation energies and charge-state transition levels of defects were calculated using 96-atom supercells, as described in Ref. 17. Wavefunctions were expanded in plane waves up to a 400 eV cutoff, and the Brillouin zone was sampled at a k -point $k = (1/4, 1/4, 1/4)$. Tests with a $2 \times 2 \times 2$ k -point mesh demonstrated convergence of transition levels to within 0.03 eV. Finite-size corrections for charged systems were applied.^{20,21}

The formation energy versus Fermi level for V_{Ga} complexed with O and/or H is plotted in Fig. 2. For a given defect, only the lowest energy charge state at each Fermi level is plotted; therefore the slope of the line segments corresponds to the charge state, and the kinks in the curves correspond to the thermodynamic charge-state transition levels (see Ref. 22 for more information and values of the transition levels). Forming a Ga vacancy results in four N dangling bonds. By adding a H, which bonds to one of the nearest-neighbor N atoms, a dangling bond is filled, and a charge-state transition level is removed from the gap.^{22,23} Similarly, replacing a nearest-neighbor N with O also removes one transition level from the gap. We will first consider V_{Ga} complexes in pure GaN and then determine the effect of adding In to form InGaN alloys.

Equation (1) applies to a defect with a single transition level; however, we see in Fig. 2 that V_{Ga} and several of its complexes have multiple transition levels in the gap of GaN (and also in InN,^{24,25} and thus in InGaN as well). Sah and Shockley²⁶ demonstrated that multiple levels can be treated sequentially, as if they were multiple defects with single transition levels. Therefore, rate equations can be solved to determine the steady-state concentration of defects in each charge state, which is needed to determine capture rates for a given carrier density.

While explicit analytical solutions can be obtained, it is even more informative to identify the rate-limiting step for SRH at these candidate defects. This can often be done by inspection of the transition level, since the order of magnitude of the nonradiative capture rate is dominated by the (roughly) exponential decrease with transition energy. For the V_{Ga} complexes with only one transition level ($V_{\text{Ga}}\text{-3H}$ and $V_{\text{Ga}}\text{-O}_\text{N}\text{-2H}$), the (+1/0) level is below mid gap and therefore holes will be captured efficiently by defects in the neutral charge state. Once this occurs, however, nonradiative electron capture will be very slow since the energy of this transition is >2.5 eV. The total recombination rate will therefore be dominated by the rate-limiting electron capture, which is more likely to occur radiatively and is therefore too slow to significantly contribute to SRH in GaN.

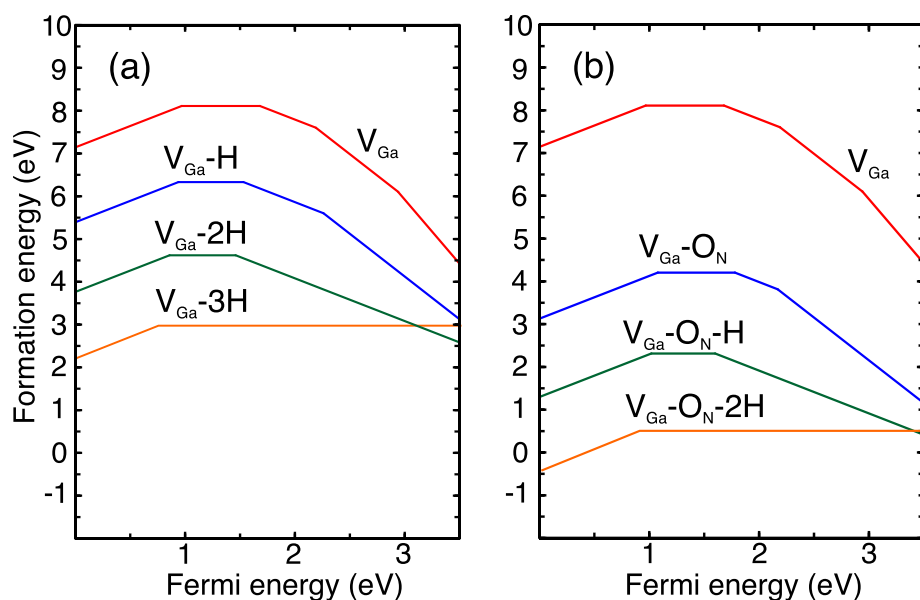


FIG. 2. Calculated formation energies of point defects in GaN as a function of Fermi energy. Ga-rich conditions are assumed, and the chemical potential of H is referenced to one half the energy of the H_2 molecule, while the chemical potential of O is referenced to the enthalpy of formation of the limiting phase Ga_2O_3 . (a) Gallium vacancy and complexes with H. (b) Gallium vacancy and complexes that involve O_N .

The same is true for the complexes with two transition levels ($V_{\text{Ga}}\text{-}2\text{H}$ and $V_{\text{Ga}}\text{-O}_\text{N}\text{-H}$, Fig. 2). Since the $(0/-1)$ transition is near mid gap, defects in the -1 charge state will capture holes fairly efficiently. Once in the neutral charge state, the defects will capture holes even more efficiently since the $(+1/0)$ level is within 1 eV of the VBM. However, for defects in the $+1$ charge state, electron capture will be very slow. Therefore, the majority of $V_{\text{Ga}}\text{-}2\text{H}$ and $V_{\text{Ga}}\text{-O}_\text{N}\text{-H}$ defects will again be “stuck” in the $+1$ charge state.

The complexes with three transition levels ($V_{\text{Ga}}\text{-H}$ and $V_{\text{Ga}}\text{-O}_\text{N}$) have an additional $(-1/-2)$ transition level relatively high in the gap. The majority of these defects will be either in the $+1$ state (since electron capture by $+1$ is very inefficient) or in the -2 state (for which hole capture is inefficient). The same argument applies to the bare V_{Ga} , most of which will be in the $+1$ or -3 charge state. From this analysis, we conclude that defects with multiple transition levels predominantly occur in the “extreme” charge states (most positive and/or most negative) and will not be efficient SRH centers.

The situation changes if capture rates are significantly enhanced for the transitions that appear as bottlenecks in the above scenarios. Since capture rates are extremely sensitive to transition energies, the shift of these energies in going from GaN to InGaN can introduce significant increases in the SRH rate. Explicit calculations of capture coefficients for a statistically meaningful set of defects in InGaN alloys are not computationally tractable; instead, we perform selected calculations and invoke knowledge about the alloy band structure^{27,28} to elucidate the effects of alloying. When considered on an absolute energy scale (i.e., with respect to the vacuum level), the reduction of the band gap with In content is reflected mainly in a lowering of the conduction-band minimum (CBM), accompanied by a much smaller upward shift of the VBM^{27,28} (see Fig. 3).

Assuming that charge-state transition levels remain approximately constant on this same absolute energy scale (as, e.g., in Ref. 29), we expect an increase in the electron

capture coefficients with In content. Electron capture was found to be the rate-limiting step for defects with one or two transition levels; in Fig. 3, we therefore focus on the examples of $V_{\text{Ga}}\text{-}3\text{H}$ and $V_{\text{Ga}}\text{-O}_\text{N}\text{-}2\text{H}$, which are also the defects with lowest formation energies (Fig. 2). Using the band alignment between InGaN alloys and GaN from Ref. 28, we observe that the energy difference between the $(+1/0)$ level and the CBM is, indeed, significantly reduced in InGaN alloys.

Our assumption that the $(+1/0)$ level remains constant at the level given by the result for the defect in pure GaN is very crude. It is to be expected that the defect properties change when the vacancy complex is embedded in InGaN, both due to the difference in lattice parameters and due to explicit interactions with In as opposed to Ga cations. Our calculations indicate that the latter effect is small: having an In atom next to a nitrogen adjacent to the vacancy affects the defect levels by at most 0.1 eV. We will show that the lattice expansion that occurs when In is added to GaN has a much bigger effect (e.g., an upward shift in the $(+1/0)$ transition level of ~ 0.8 eV for 50% In, compared to a constant level).

Given the insensitivity to the explicit presence of In, we have simulated this effect by calculating the defects in a GaN supercell with lattice parameters expanded to match the volume of InGaN alloys with 5%, 10%, 20%, and 50% In. To apply this information to actual InGaN alloys, we align VBM_{avg} in the expanded cell with that of unstrained GaN using the absolute valence-band deformation potential of GaN.³⁰ This results in the green dot-dashed line in Fig. 3, which shows that the $(+1/0)$ level moves significantly closer to the CBM in the InGaN alloys.

We have verified this approach by comparing with explicit calculations for defects in InGaN supercells at selected alloy compositions. These calculations also allow us to evaluate the changes in other parameters that determine nonradiative capture.¹⁰ The volume expansion in InGaN alloys decreases the frequency of the vibrational mode that couples to the deformation between the structure of the 0 and

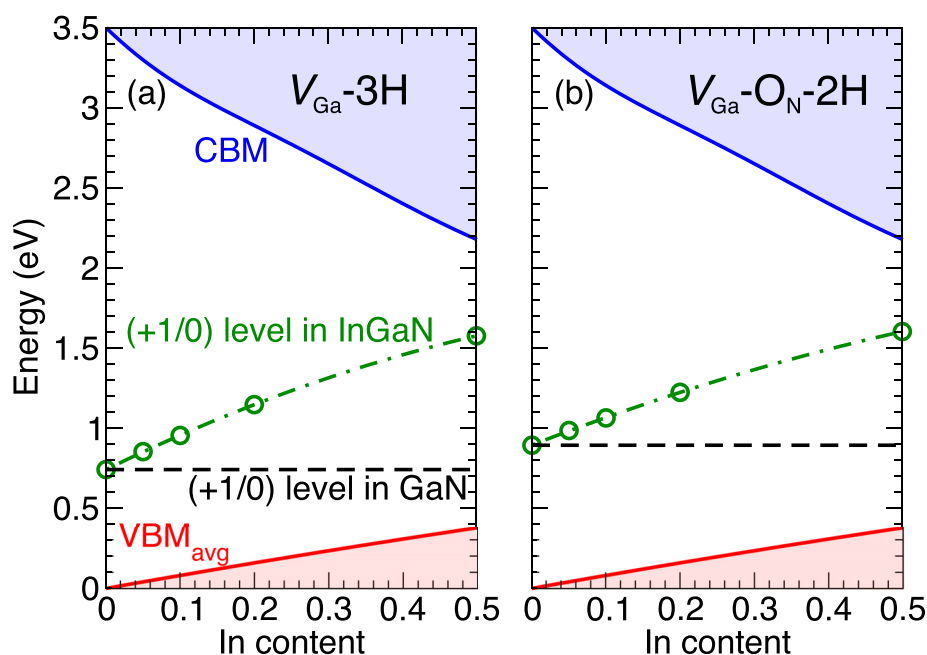


FIG. 3. Position of the $(+1/0)$ transition level within the band gap of InGaN as a function of In content for (a) the $V_{\text{Ga}}\text{-}3\text{H}$ and (b) the $V_{\text{Ga}}\text{-O}_\text{N}\text{-}2\text{H}$ complex. For the valence band, an average over the top three valence bands is shown.^{27,28} VBM_{avg} of bulk GaN was chosen as the reference energy. The black dashed line assumes the transition level is constant on an absolute energy scale and given by the value in GaN; the green dot-dashed line takes the change in volume of the InGaN alloy into account, interpolating between the explicit calculations given by the green circles.

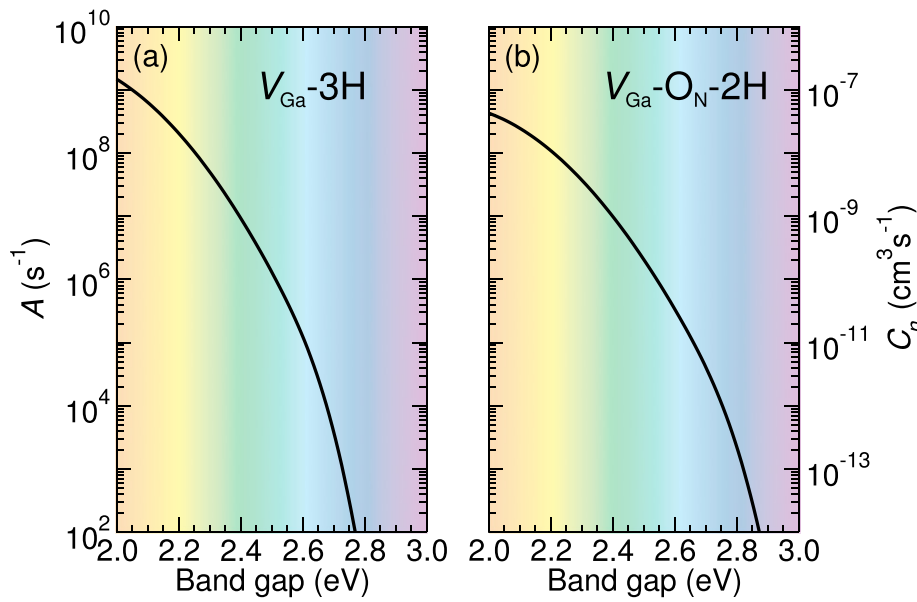


FIG. 4. SRH A coefficient for the (a) $V_{\text{Ga}}\text{-3H}$ and (b) $V_{\text{Ga}}\text{-O}_\text{N}\text{-2H}$ complexes versus band gap of the InGa N alloy, assuming a defect density of 10^{16} cm^{-3} and a temperature of 120°C . As electron capture is the rate-limiting step, A is proportional to C_n , which is shown on the right vertical axis. The color spectrum indicates the corresponding wavelengths of light.

+1 charge states, and increases the amount of lattice relaxation between them. This results in an increase in the capture coefficient by a factor of two for 20% InGa N , i.e., a small effect compared to the (exponential) changes induced by the change in the transition energy. In the following calculations of capture coefficients, we have therefore used the vibrational frequency and lattice relaxation reported in Ref. 22 for pure Ga N .

In Fig. 4, we plot the A coefficient [Eq. (1)] vs. the band gap of InGa N for $V_{\text{Ga}}\text{-3H}$ and $V_{\text{Ga}}\text{-O}_\text{N}\text{-2H}$ complexes (assuming $N = 10^{16}\text{ cm}^{-3}$). The temperature was set to $T = 120^\circ\text{C}$, a typical internal temperature of operating LEDs.³¹ The electron capture process, though significantly enhanced in InGa N alloys compared to bulk Ga N , is still the rate-limiting step and therefore $A \simeq NC_n$.

Figure 4 shows that the SRH coefficients for $V_{\text{Ga}}\text{-3H}$ and $V_{\text{Ga}}\text{-O}_\text{N}\text{-2H}$ behave similarly. For band gaps in the green (around 2.4 eV), the SRH coefficient is of the order 10^7 s^{-1} , consistent with A values obtained from fitting to experimental data.¹³ At typical operating carrier densities of around $n = 10^{18}\text{ cm}^{-3}$ (Ref. 4), this will result in a SRH rate $R_{\text{SRH}} = An = 10^{25}\text{ cm}^{-3}\text{ s}^{-1}$. Radiative band-to-band recombination coefficients in Ga N and InGa N are of the order $B = 4 \times 10^{-11}\text{ cm}^3\text{ s}^{-1}$,^{4,5} so the radiative recombination rate will be $R_{\text{rad}} = Bn^2 = 4 \times 10^{25}\text{ cm}^{-3}\text{ s}^{-1}$. A value of $R_{\text{SRH}} = 10^{25}\text{ cm}^{-3}\text{ s}^{-1}$ thus implies that approximately 20% of the carriers will be lost through SRH recombination. Since the rates increase for alloys with band gaps in the yellow (2.1–2.2 eV), the concentration of a defect with this rate would have to be kept below 10^{15} cm^{-3} for the device to emit light at all.

The structures and transition energy for the (+1/0) level of $V_{\text{Ga}}\text{-2H}$ are very similar to those for $V_{\text{Ga}}\text{-3H}$; the same applies to $V_{\text{Ga}}\text{-O}_\text{N}\text{-H}$ compared to $V_{\text{Ga}}\text{-O}_\text{N}\text{-2H}$. Since the rate-limiting step is the same in all these complexes, we expect that the $V_{\text{Ga}}\text{-2H}$ and $V_{\text{Ga}}\text{-O}_\text{N}\text{-H}$ complexes will have SRH A coefficients similar to their counterparts in Fig. 4.

The high SRH recombination rates associated with these V_{Ga} -related complexes would thus appear to be detrimental, since their formation energy (Fig. 2) is quite low. There is a

mitigating factor, however. In most optoelectronic devices, the InGa N quantum wells are under biaxial stress, with the a lattice constant constrained to match that of Ga N . Preliminary calculations for defects in biaxially stressed InGa N indicate that the A coefficients are lower by one to two orders of magnitude. Maintaining the coherence of the InGa N layers during epitaxial growth is thus essential, since relaxation towards the bulk lattice parameters will lead to an increase in the A coefficient for a given In content. Our observations also indicate that judicious engineering of stress could provide a means of suppressing nonradiative recombination. Finally, our work also highlights the importance of controlling oxygen incorporation during growth, since the gallium-vacancy-related complexes form especially easily in the presence of oxygen (Fig. 2).

In summary, we have used first-principles calculations of transition levels and capture coefficients to demonstrate that $V_{\text{Ga}}\text{-3H}$, $V_{\text{Ga}}\text{-O}_\text{N}\text{-2H}$, $V_{\text{Ga}}\text{-2H}$, and $V_{\text{Ga}}\text{-O}_\text{N}\text{-H}$ complexes are efficient SRH centers and potentially detrimental for InGa N alloys with band gaps in the green and yellow. Depending on the wavelength and stress state of the InGa N layer, concentrations of 10^{16} cm^{-3} can result in SRH nonradiative recombination on the same order as radiative recombination, severely reducing the IQE of the device.

We acknowledge M. A. Reshchikov, C. Weisbuch, J. Shen, and Q. Yan for fruitful interactions. This work was supported by the U. S. Department of Energy (DOE), Office of Science, Basic Energy Sciences, under Award No. DE-SC0010689. A.A. was supported by Marie Skłodowska-Curie Action of the European Union (project Nitride-SRH, Grant No. 657054). Computational resources were provided by the National Energy Research Scientific Computing Center, supported by the DOE Office of Science under Contract No. DE-AC02-05CH11231.

¹S. Nakamura and M. R. Krames, *Proc. IEEE* **101**, 2211 (2013).

²W. Shockley and W. T. Read, *Phys. Rev.* **87**, 835 (1952).

³R. N. Hall, *Phys. Rev.* **87**, 387 (1952).

⁴A. David and M. J. Grundmann, *Appl. Phys. Lett.* **97**, 033501 (2010).

- ⁵E. Kioupakis, Q. Yan, D. Steiauf, and C. G. Van de Walle, *New J. Phys.* **15**, 125006 (2013).
- ⁶H. Nykänen, S. Suihkonen, L. Kilanski, M. Sopanen, and F. Tuomisto, *Appl. Phys. Lett.* **100**, 122105 (2012).
- ⁷A. Hierro, S. A. Ringel, M. Hansen, J. S. Speck, U. K. Mishra, and S. P. DenBaars, *Appl. Phys. Lett.* **77**, 1499 (2000).
- ⁸S. F. Chichibu, A. Uedono, T. Onuma, T. Sota, B. A. Haskell, S. P. Denbaars, J. S. Speck, and S. Nakamura, *Appl. Phys. Lett.* **86**, 021914 (2005).
- ⁹A. Uedono, K. Tenjinbayashi, T. Tsutsui, Y. Shimahara, H. Miyake, K. Hiramatsu, N. Oshima, R. Suzuki, and S. Ishibashi, *J. Appl. Phys.* **111**, 013512 (2012).
- ¹⁰A. Alkauskas, Q. Yan, and C. G. Van de Walle, *Phys. Rev. B* **90**, 075202 (2014).
- ¹¹C. Henry and D. Lang, *Phys. Rev. B* **15**, 989 (1977).
- ¹²E. C. H. Kyle, S. W. Kaun, P. G. Burke, F. Wu, Y.-R. Wu, and J. S. Speck, *J. Appl. Phys.* **115**, 193702 (2014).
- ¹³J. Danhof, U. T. Schwarz, T. Meyer, C. Vierheilg, and M. Peter, *Phys. Status Solidi B* **249**, 600 (2012).
- ¹⁴W. G. Scheibenzuber, U. T. Schwarz, L. Sulmoni, J. Dorsaz, J.-F. Carlin, and N. Grandjean, *J. Appl. Phys.* **109**, 093106 (2011).
- ¹⁵M. A. Reschikov, *AIP Conf. Proc.* **1583**, 127 (2014).
- ¹⁶A. Alkauskas, J. L. Lyons, D. Steiauf, and C. G. Van de Walle, *Phys. Rev. Lett.* **109**, 267401 (2012).
- ¹⁷C. Freysoldt, B. Grabowski, T. Hickel, G. Kresse, A. Janotti, J. Neugebauer, and C. G. Van de Walle, *Rev. Mod. Phys.* **86**, 253 (2014).
- ¹⁸G. Kresse and J. Furthmüller, *Phys. Rev. B* **54**, 11169 (1996); G. Kresse and D. Joubert, *Phys. Rev. B* **59**, 1758 (1999).
- ¹⁹J. Heyd, G. E. Scuseria, and M. Ernzerhof, *J. Chem. Phys.* **118**, 8207 (2003).
- ²⁰C. Freysoldt, J. Neugebauer, and C. G. Van de Walle, *Phys. Rev. Lett.* **102**, 016402 (2009).
- ²¹C. Freysoldt, J. Neugebauer, and C. G. Van de Walle, *Phys. Status Solidi B* **248**, 1067 (2011).
- ²²J. L. Lyons, A. Alkauskas, A. Janotti, and C. G. Van de Walle, *Phys. Status Solidi B* **252**, 900 (2015).
- ²³C. G. Van de Walle, *Phys. Rev. B* **56**, R10020 (1997).
- ²⁴C. G. Van de Walle, J. L. Lyons, and A. Janotti, *Phys. Status Solidi A* **207**, 1024 (2010).
- ²⁵X. M. Duan and C. Stampfl, *Phys. Rev. B* **79**, 035207 (2009).
- ²⁶C.-T. Sah and W. Shockley, *Phys. Rev.* **109**, 1103 (1958).
- ²⁷P. G. Moses and C. G. Van de Walle, *Appl. Phys. Lett.* **96**, 021908 (2010).
- ²⁸P. G. Moses, M. Miao, Q. Yan, and C. G. Van de Walle, *J. Chem. Phys.* **134**, 084703 (2011).
- ²⁹J. L. Lyons, A. Janotti, and C. G. Van de Walle, *Phys. Rev. B* **89**, 035204 (2014).
- ³⁰C. G. Van de Walle and J. Neugebauer, *Appl. Phys. Lett.* **70**, 2577 (1997).
- ³¹C.-C. Pan, T. Gilbert, N. Pfaff, S. Tanaka, Y. Zhao, D. Feezell, J. S. Speck, S. Nakamura, and S. P. DenBaars, *Appl. Phys. Express* **5**, 102103 (2012).